

Activity-Dependent Release of Tissue Plasminogen Activator from the Dendritic Spines of Hippocampal Neurons Revealed by Live-Cell Imaging

Janis E. Lochner,^{1,2} Leah S. Honigman,² Wilmon F. Grant,² Sarah K. Gessford,²
Alexis B. Hansen,² Michael A. Silverman,^{3*} and Bethe A. Scalettar⁴

¹ Department of Chemistry, Lewis & Clark College, Portland, Oregon 97219

² Program in Biochemistry and Molecular Biology, Lewis & Clark College, Portland, Oregon 97219

³ Center for Research on Occupational and Environmental Toxicology, Oregon, Health Sciences University, Portland, Oregon 97239

⁴ Department of Physics, Lewis & Clark College, Portland, Oregon 97219

Received 6 September 2005; accepted 7 November 2005

ABSTRACT: Tissue plasminogen activator (tPA) has been implicated in a variety of important cellular functions, including learning-related synaptic plasticity and potentiating *N*-methyl-D-aspartate (NMDA) receptor-dependent signaling. These findings suggest that tPA may localize to, and undergo activity-dependent secretion from, synapses; however, conclusive data supporting these hypotheses have remained elusive. To elucidate these issues, we studied the distribution, dynamics, and depolarization-induced secretion of tPA in hippocampal neurons, using fluorescent chimeras of tPA. We found that tPA resides in dense-core granules (DCGs) that traffic to post-synaptic dendritic spines and that can remain in spines for extended periods. We also found that depolarization induced by high potassium levels elicits a slow, partial exo-

cytic release of tPA from DCGs in spines that is dependent on extracellular Ca^{+2} concentrations. This slow, partial release demonstrates that exocytosis occurs via a mechanism, such as fuse-pinch-linger, that allows partial release and reuse of DCG cargo and suggests a mechanism that hippocampal neurons may rely upon to avoid depleting tPA at active synapses. Our results also demonstrate release of tPA at a site that facilitates interaction with NMDA-type glutamate receptors, and they provide direct confirmation of fundamental hypotheses about tPA localization and release that bear on its neuromodulatory functions, for example, in learning and memory. © 2006

Wiley Periodicals, Inc. *J Neurobiol* 66: 564–577, 2006

Keywords: tPA; dense-core granule; regulated secretion; hippocampus; synaptic plasticity

*Present address: Department of Biology, Simon Fraser University, Burnaby, British Columbia, V5A 1S6, Canada.

Correspondence to: J.E. Lochner (lochner@lclark.edu).

Contract grant sponsor: National Institutes of Health; contract grant numbers: 1 R15 NS40425-01 (J.E.L.), 1 R15 GM061539-01 (B.A.S.), and MH 66179 (to Dr. Gary Banker of Oregon Health Sciences University).

© 2006 Wiley Periodicals, Inc.

Published online 22 March 2006 in Wiley InterScience (www.interscience.wiley.com).

DOI 10.1002/neu.20250

INTRODUCTION

Long-term memory formation involves the establishment of enduring changes in synaptic connections. These changes are mediated largely by the activity of specific proteins (Kandel, 2001). Many of the proteins that mediate changes in the strength of synaptic connections (i.e., synaptic plasticity) have been identified (Qian et al., 1993; Patterson et al., 1996;

Guzowski et al., 2000). Prominent among these is the serine protease tissue plasminogen activator (tPA), a protein best known for the role that it plays in plasmin-mediated degradation of fibrin-containing blood clots.

A considerable body of data implicates tPA in learning-related synaptic plasticity. For example, regions of the adult brain that exhibit activity-dependent structural plasticity, the hippocampus, cerebellum, and amygdala, express tPA (Sappino et al., 1993; Davies et al., 1998; Salles and Strickland, 2002; Pawlak et al., 2003). Moreover, during activity-dependent forms of synaptic plasticity, such as the active phase of cerebellar motor skill learning, tPA mRNA and protein are induced in Purkinje neurons (Seeds et al., 1995, 2003).

Studies of long-term potentiation (LTP), a cellular model of learning induced by short, high-frequency electrical stimuli, also implicate tPA in synaptic plasticity. Specifically, tPA mRNA is induced during the late phase of LTP (L-LTP) (Qian et al., 1993). Moreover, mice in which the tPA gene is ablated show a selective defect in L-LTP (Frey et al., 1996; Huang et al., 1996), whereas transgenic mice in which tPA expression is augmented show enhanced L-LTP (Madani et al., 1999).

Several molecular mechanisms have been advanced to explain how tPA may act to modulate synaptic transmission and plasticity. For example, tPA, which is secreted by neurons (Gualandris et al., 1996; Baranes et al., 1998; Fernandez-Monreal et al., 2004b), could influence plasticity through its role in converting extracellular plasminogen into the active protease plasmin. Plasmin then could reshape synapses by degrading extracellular matrix components (Hoffman et al., 1998; Endo et al., 1999; Nakagami et al., 2000; Wu et al., 2000), thereby facilitating axonal elongation and synaptic growth (Baranes et al., 1998). Alternatively, plasmin could convert the precursor of brain-derived neurotrophic factor (BDNF) into mature BDNF, and BDNF then could produce enduring changes in synaptic organization (Pang et al., 2004). BDNF is known to stimulate the growth of dendritic spines, augment synapse density, and elicit long-lasting enhancement of synaptic transmission (Lessmann et al., 1994; Levine et al., 1995; Li et al., 1998; Tyler and Pozzo-Miller, 2001, 2003).

tPA also could influence plasticity by modulating intracellular signaling events (Zhuo et al., 2000). In support of this possibility, tPA interacts with cell surface proteins, including the *N*-methyl-D-aspartate (NMDA) receptor and the low-density lipoprotein receptor-related protein (LRP), and thereby activates signaling pathways involved in learning. In the case of the NMDA receptor, tPA binding leads to a poten-

tiated Ca^{+2} influx and enhanced NMDA receptor-mediated signaling (Nicole et al., 2001; Matys and Strickland, 2003; Fernandez-Monreal et al., 2004a,b); tPA binding to the NMDA receptor also leads to activation of the extracellular-regulated kinase signal transduction pathway (Medina et al., 2005), which is critical for activity-dependent dendritic plasticity in hippocampal neurons (Wu et al., 2001; Alonso et al., 2004). In the case of LRP, tPA binding leads to activation of protein kinase A signaling pathways, which play a key role in L-LTP (Zhuo et al., 2000).

In models of tPA-mediated synaptic plasticity, tPA is presumed to be strategically positioned at synapses and poised for activity-dependent release from synaptic structures. However, synaptic release of tPA has never been directly demonstrated, and fundamental questions regarding the nature of the release event remain unanswered. For example, how is tPA positioned and housed at synaptic structures? What are the kinetics and extent of release of tPA in response to synaptic stimulation? In the present study, we developed a system for visualizing tPA at synaptic structures in living hippocampal neurons. Using wide-field fluorescence microscopy and fluorescent tPA chimeras, we demonstrate that tPA resides in dense-core granules (DCGs) that traffic to dendritic spines and that are retained in spines for extended periods prior to depolarization-induced exocytosis. Release of tPA from dendritic spines is critically dependent on extracellular Ca^{+2} , and the exocytotic event triggered by depolarization leads only to a partial release of tPA. These results provide direct confirmation of fundamental hypotheses about tPA distribution and secretion that bear on its function in synaptic plasticity, and they suggest that tPA that resides within DCGs in spines is available for multiple cycles of synaptic release.

METHODS

Viral Infection of Primary Cultures of Hippocampal Neurons

Low density primary cultures of dissociated neurons from embryonic day 18 rat hippocampi were prepared essentially as described previously (Banker and Goslin, 1998). To facilitate neuronal expression of the fluorescent proteins, tPA-EGFP, tPA-EYFP, and ECFP, the gene for each of these proteins was packaged into a replication-deficient herpes simplex and the viruses were used to deliver DNA into neurons (Ho, 1994). The rat tPA gene used in these constructs contained the complete coding sequence for the protein as well as the coding information for the tPA signal sequence. Past work indicated that the signal sequence was required to target tPA to DCGs (Lochner et al., 1998). Hippocampal cultures were infected with the viral expression

vectors after mature glutamatergic synapses had formed, typically between 14–18 days *in vitro* (DIV). Cultures were used for either live-imaging or immunostaining of relevant proteins 24–28 h postinfection.

Immunofluorescence Staining

Immunostaining was used to identify carrier organelles for tPA chimeras in mature hippocampal neurons, to determine the axonal and dendritic distribution of tPA chimeras in mature hippocampal neurons, and to determine if tPA chimeras are present in synapses in mature hippocampal neurons. In preparation for immunostaining, virally infected hippocampal neurons growing on cover-slips were fixed with 4% paraformaldehyde and permeabilized with 0.25% Triton X-100, as described previously (Withers et al., 2000). To identify carrier organelles for tPA, fixed neurons expressing tPA-EGFP were immunostained with an affinity-purified rabbit polyclonal antibody against the endogenous DCG protein secretogranin II (SgII) (a gift from Dr. Patrizia Rosa, CNR, Milan, Italy), as described previously (Silverman et al., 2005). To quantify the distribution of tPA chimeras in axons and dendrites, neurons expressing tPA-EGFP were immunostained similarly with a rabbit primary antiserum against the dendritic marker MAP2 (a gift from Dr. Shelley Halpain, Scripps Research Institute, San Diego, CA) and a monoclonal antibody against the axonal marker tau-1 (a gift from Dr. T. Frankfurter, University of Virginia, Charlottesville, VA). Finally, to determine if tPA chimeras localize in synapses, neurons expressing tPA-EYFP and ECFP were immunostained with an affinity-purified rabbit polyclonal against the presynaptic marker synapsin-1 (a gift from Dr. Gary Banker, Oregon Health Sciences University, Portland, OR).

Imaging

Fluorescence microscopy was used to study the distribution and dynamics of DCGs containing tPA chimeras in hippocampal neurons. Images were collected on a Leica microscope (Leica Microsystems, Chantilly, VA) under the control of MetaMorph software (Universal Imaging, Downingtown, PA). Most static images of distribution in fixed cells were generated by optically sectioning cells in 0.2 μm focal increments (Hiraoka et al., 1991; Scalettar et al., 1996); these images were deblurred using a constrained iterative deconvolution algorithm to improve their clarity (Scalettar et al., 1996). Time-lapse images of living cells were collected every 0.5–30 s from a single focal plane; these images also were deblurred to improve their clarity and to facilitate tracking of DCGs.

Release Assays

To determine if tPA-EYFP was released from a site, such as a dendritic spine, cover-slips containing hippocampal neurons expressing tPA-EYFP and ECFP were mounted in a series-20 perfusion chamber (Warner Instrument Corpora-

tion) that was maintained at 32°C. A cover-slip was scanned and dual-color (yellow and cyan) images were collected and examined visually to locate neurons in which tPA-EYFP was present at the relevant site.

Depolarization-induced release of tPA-EYFP from sites was assayed by first imaging cells in a low-potassium HEPES buffer (100 mM NaCl, 4 mM KCl, 20 mM HEPES, pH 7.3, 2 mM CaCl₂, 1 mM MgCl₂, 10 mM glucose, 0.01 mM glycine, pH 7.3). This buffer then was replaced with a depolarizing, high-potassium HEPES buffer (54 mM NaCl, 50 mM KCl, 20 mM HEPES, pH 7.3, 2 mM CaCl₂, 1 mM MgCl₂, 10 mM glucose, 0.01 mM glycine, pH 7.3) using tubing connected to a buffer reservoir. Cells then were imaged every 30 s from 1 to 10 min after addition of the high KCl buffer. To assay the effects of photobleaching on fluorescence signals, cells were imaged similarly without replacing the low-potassium buffer. To assay the calcium dependence of release, the high-KCl HEPES buffer was modified so that Ca⁺² was replaced by Mg⁺² and 5 mM EGTA was added.

Data Analysis

Quantification of Release. Loss of tPA-EYFP fluorescence induced by depolarization was determined by calculating and comparing fluorescence signals emitted by DCGs before and after addition of high KCl. Fluorescence signals emitted by DCGs were calculated by generating background-subtracted images and then outlining the DCGs and computing average intensities inside the outlined areas, using the public domain program ImageJ.

Tracking. DCGs were tracked laterally in two dimensions (x,y) in background-subtracted movies using ImageJ. Tracking involved manually surrounding a DCG in a given frame with a circle of diameter $\approx 0.7 \mu\text{m}$ and calculating the center of mass of the fluorescence distribution in the circle using ImageJ. In some cases, a noncircular region was used, because movement during an exposure would cause a DCG to appear noncircular in shape. Tracking of a DCG in successive frames was continued as long as the DCG could be identified unambiguously. The (x,y) coordinates of the centers of mass of DCGs were tabulated as a function of frame number and converted into trajectories, as described previously (Abney et al., 1999).

Quantification of Speeds and Diffusion Coefficients. Lateral DCG motion was characterized quantitatively by computing the mean-squared displacement, $\langle r^2 \rangle$, of DCGs as a function of time, t , and fitting to a model that describes “diffusive” and “directed” motion as follows (Saxton and Jacobson, 1997; Abney et al., 1999):

$$\langle r^2(t) \rangle = 4Dt + v^2t^2 \quad (1)$$

Here, r is displacement, D is the diffusion coefficient, and v is speed; brackets denote averaging, which was performed as described previously (Abney et al., 1999). In eq. (1), dif-

fusive motion produces a linear relationship between $\langle r^2 \rangle$ and t , whereas directed motion produces a linear relationship between $\langle r^2 \rangle^{1/2}$ and t . D 's and v 's were computed from fits to eq. (1), as described previously (Abney et al., 1999).

DCGs were characterized as effectively laterally immobile if their associated diffusion coefficients were very small ($D \leq 5.0 \times 10^{-12} \text{ cm}^2/\text{s} = 5.0 \times 10^{-4} \mu\text{m}^2/\text{s}$), similar to previous work (Burke et al., 1997; Silverman et al., 2005).

Quantification of Data Statistics. Statistical data are reported either as a mean \pm standard deviation (SD) or as a mean \pm standard error of the mean (SEM). Statistical similarities and differences between data were analyzed using the Student's t test function in Excel and are reported in terms of p values (Microsoft, Redmond, WA). For the t test analysis, we adopted standard criteria and assumed that two data sets were statistically different if $p < 0.05$ and were statistically similar if $p > 0.05$.

RESULTS

To visualize tPA in hippocampal neurons, we constructed a replication defective herpes simplex-1 virus (HSV-1) that facilitates expression and visualization of a fluorescent fusion protein consisting of rat tPA and EGFP (tPA-EGFP) in mature, living, and fixed hippocampal neurons.

tPA-EGFP Localizes to DCGs in Mature Cultures of Hippocampal Neurons

We first identified the carrier organelle for tPA-EGFP in mature hippocampal neurons. Fluorescent tPA chimeras localize to DCGs in neuroendocrine cells (Lochner et al., 1998; Taraska et al., 2003) and in developing hippocampal neurons (Silverman et al., 2005). Several lines of evidence suggest that this also is the case for mature hippocampal neurons. First, in mature hippocampal neurons, tPA-EGFP produces punctate fluorescence throughout the neuronal processes, as well as bright staining of the Golgi apparatus, consistent with packaging of tPA-EGFP into DCGs [Fig. 1(A)]. Second, in mature hippocampal neurons, tPA-EGFP colocalizes extensively with SgII, an established marker for DCGs. Figure 1(B) shows a subregion of a process of a 14 DIV hippocampal neuron expressing tPA-EGFP that was immunostained for endogenous SgII. In this image, all seven of the organelles containing tPA-EGFP also stained for SgII; on average, $81 \pm 2\%$ (SD) of organelles containing tPA-EGFP also stained for endogenous SgII in mature hippocampal neurons ($n = 2$ cells; 103 puncta).

DCGs Containing tPA Chimeras Localize Extensively within Dendrites

We next determined the distribution of DCGs containing tPA-EGFP within axonal and dendritic processes of mature hippocampal neurons. To this end, we used immunostaining to label the dendritic constituent, microtubule associated protein (MAP-2), and to label the axonal constituent, tau-1, in neurons expressing tPA-EGFP. Figure 1(C,D) shows that tPA-EGFP is present in both dendrites and axons. However, because the dendritic arbor is so expansive, $92 \pm 3\%$ (SD) of DCGs containing tPA-EGFP were present in dendrites ($n = 3$ cells; 3783 puncta). Similar results hold for DCGs containing BDNF in hippocampal neurons (Haubensak et al., 1998; Hartmann et al., 2001).

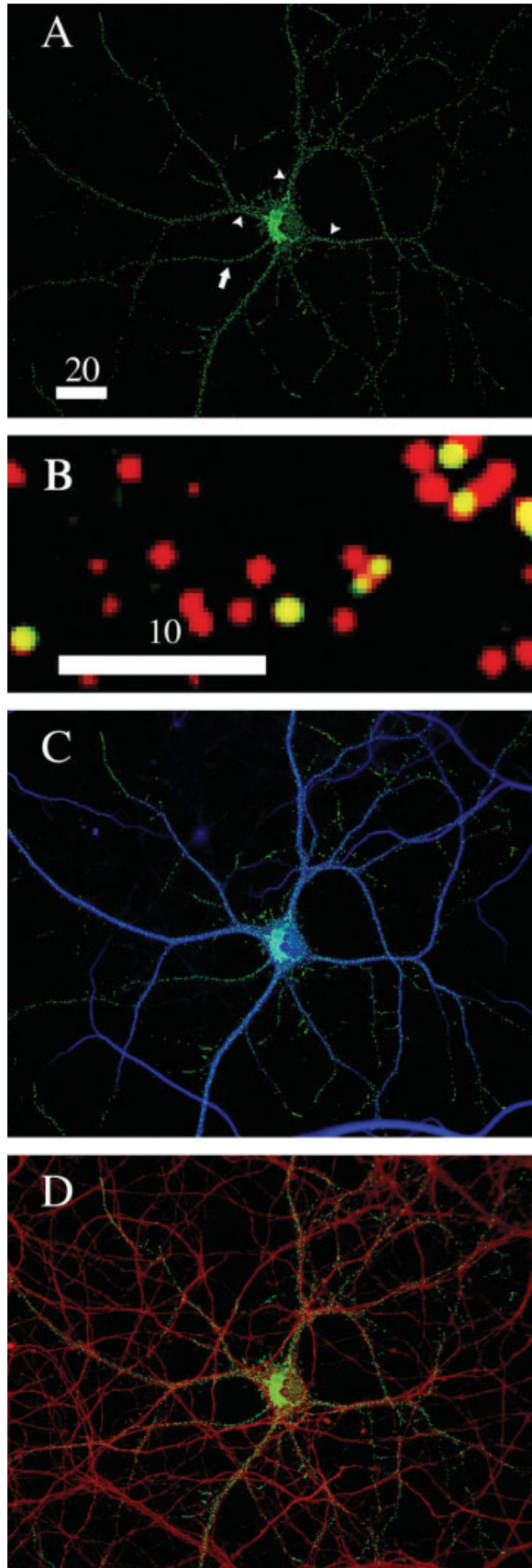
DCGs Containing tPA Chimeras Are Present in Dendritic Spines

Because DCGs containing tPA-EGFP are found extensively in dendrites, and because tPA is hypothesized to be a postsynaptic communicator in memory formation (Zhuo et al., 2000), we next developed a system suited to elucidating the postsynaptic localization of tPA chimeras. Specifically, we created two additional HSV-1 viruses, tPA-EYFP and ECFP, and used these viruses to visualize tPA at postsynaptic sites. In our system, ECFP reveals neuronal morphology, notably dendritic spine morphology, because it diffuses freely throughout neurons, and tPA-EYFP reveals the distribution of tPA without spectral overlap from ECFP.

Figure 2 shows that DCGs containing tPA-EYFP were present in dendritic spines of mature hippocampal neurons; quantification revealed that 31% of spines contained at least one DCG containing tPA-EYFP ($n = 356$ spines). DCG position within the spine varied: $\approx 50\%$ of spines contained at least one DCG containing tPA-EYFP in the stalk of the spine, and $\approx 50\%$ of spines contained at least one DCG containing tPA-EYFP in the head of the spine.

DCGs Containing tPA Chimeras Are Present Preferentially in Dendritic Spines Apposed to Presynaptic Sites

Recent data indicate that not all spines in hippocampal neurons are apposed to a cluster of synaptobrevin-immunostained synaptic vesicles (SVs), suggesting that not all spines are synapsed with a preterminal partner (Tyler and Pozzo-Miller, 2001). Given this, we immunostained neurons expressing tPA-EYFP



and ECFP with an antibody against the preterminal marker synapsin I to determine the distribution of tPA-EYFP in spines that were synapsed with a preterminal partner.

Figure 3 shows that DCGs containing tPA-EYFP localized to synapsed spines. Moreover, quantification revealed that DCGs containing tPA-EYFP preferentially localized to synapsed spines. Specifically, DCGs containing tPA-EYFP were present in 49% of spines that were synapsed but in only 16% of spines that were not synapsed ($n = 356$ spines). In addition, 51% of the synapsed spines that contained tPA-EYFP contained multiple DCGs containing tPA-EYFP.

DCGs Containing tPA-EYFP Are Retained in Spines for Long Amounts of Time

Our static images demonstrate that DCGs containing tPA-EYFP were present at postsynaptic sites. However, these images did not reveal whether DCGs in spines were retained at this critical release site for long amounts of time in preparation for exocytosis, similar to SVs (Kraszewski et al., 1995, 1996; Henkel et al., 1996; Zenisek et al., 2000). To address this issue, we tracked DCGs present in the dendritic spines of living hippocampal neurons ($n = 62$ DCGs).

Figure 4(A) shows a representative trajectory of a DCG in a spine, superimposed on an outline of the spine; an associated movie can be viewed at <http://www.lclark.edu/~lochner/DCG.html>. This trajectory, and the movie, both suggest that the DCG was nearly immobile.

To determine the percentage of DCGs in spines that were immobile, and to elucidate mechanisms of motion for DCGs in spines that were mobile, we generated plots of $\langle r^2 \rangle^{1/2}$ versus t and $\langle r^2 \rangle$ versus t . Linearity of the $\langle r^2 \rangle^{1/2}$ plot revealed directed motion,

Figure 1 tPA-EGFP localizes to DCGs that are distributed in the axonal and dendritic processes of mature hippocampal neurons. Deblurred fluorescence images (A) of a 16-DIV hippocampal neuron expressing tPA-EGFP, and (B) of a subregion of a process of a 14-DIV hippocampal neuron expressing tPA-EGFP (green) and immunostained for endogenous SgII (red). In panel (B), all tPA-EGFP-containing organelles also stained for SgII and thus appear yellow. Immunofluorescence labeling (C) of the dendritic marker protein MAP-2 (blue), and (D) of the axonal marker protein tau-1 (red) revealed the distribution of tPA-EGFP-containing DCGs (green) in axons and dendrites. Arrow indicates the axon and arrowheads indicate the dendrites. Bars = 10 and 20 μm .

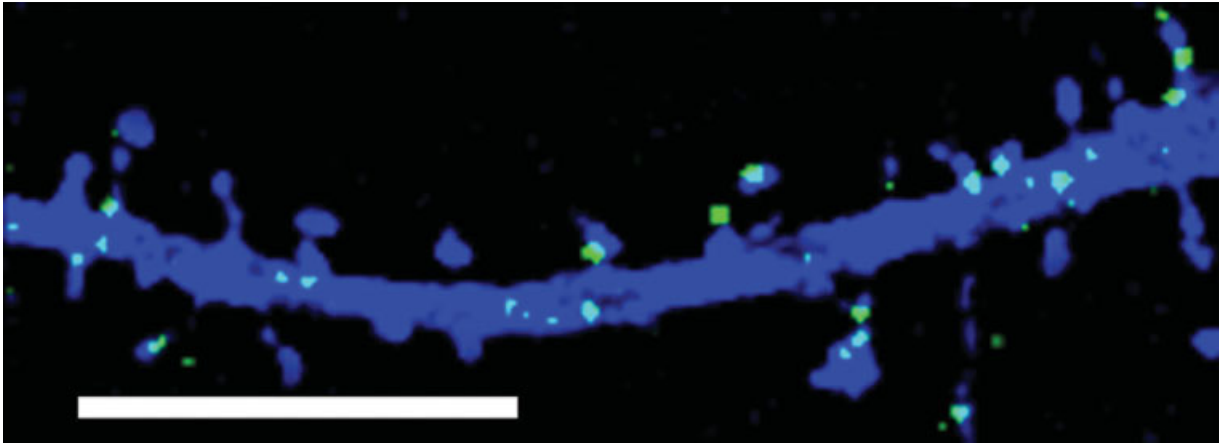


Figure 2 tPA-EYFP-containing DCGs are present in dendritic spines. Dual-color image showing the distribution of tPA-EYFP-containing DCGs in the spines and associated dendritic process of a 14-DIV hippocampal neuron following 24 h expression of ECFP (blue) and tPA-EYFP (yellow). Bar = 20 μm .

whereas linearity of the $\langle r^2 \rangle$ plot revealed diffusive motion; in addition, a sufficiently small plot slope (e.g., diffusion coefficient) revealed immobility.

Figure 4(B,C) quantifies mobility rigorously, showing representative plots of $\langle r^2 \rangle^{1/2}$ versus t (B) and $\langle r^2 \rangle$ versus t (C) that were derived from trajectories of three DCGs in spines, including the DCG shown in Figure 4(A). These plots reveal that $\langle r^2 \rangle$ varies linearly with t , implying that the “motion” of the DCGs was diffusive. In the case of the DCG in Figure 4(A), the diffusion coefficient computed from the slope of the $\langle r^2 \rangle$ versus t plot was very small, $D = 5.3 \times 10^{-12} \text{ cm}^2/\text{s}$, demonstrating that the DCG was nearly immobile. In the case of the two other DCGs, $D = 1.1 \times 10^{-12} \text{ cm}^2/\text{s}$ and $D = 2.3 \times 10^{-11} \text{ cm}^2/\text{s}$, demonstrating that these DCGs were truly immobile and slowly mobile. Additional tracking and quantification revealed that 77% of DCGs in spines were immobile ($n = 62$ DCGs). This suggests that most DCGs, like SVs, are retained at pivotal release sites, such as dendritic spines, in preparation for exocytosis.

For comparative purposes, we also tracked DCGs in processes ($n = 70$ DCGs). Tracking in processes also is of intrinsic interest. For example, it reveals how quickly DCGs containing tPA-EYFP can reach spines following their synthesis in the soma. The efficient delivery of tPA to active synapses has recently been experimentally explored (Shin et al., 2004) and is considered more fully in the Discussion.

DCGs in processes are highly mobile, unlike DCGs in spines. Figure 5(A) shows several representative trajectories of DCGs in processes, together with comparative trajectories in spines, superimposed on an outline of the processes and spines. These trajectories

suggest that DCGs in processes frequently undergo fast, directed transport, unlike DCGs in spines.

Figure 5(B,C) illustrates the attributes of DCG mobility in processes quantitatively, showing representative plots of $\langle r^2 \rangle^{1/2}$ versus t (B) and $\langle r^2 \rangle$ versus t (C) that were derived from trajectories of DCGs in Figure 5(A). For DCGs A and B, which appear to have undergone rapid and directed motion, $\langle r^2 \rangle^{1/2}$ varies linearly with t , implying that the motion of these DCGs was directed. In contrast, for DCGs C and D, which appear to have undergone random

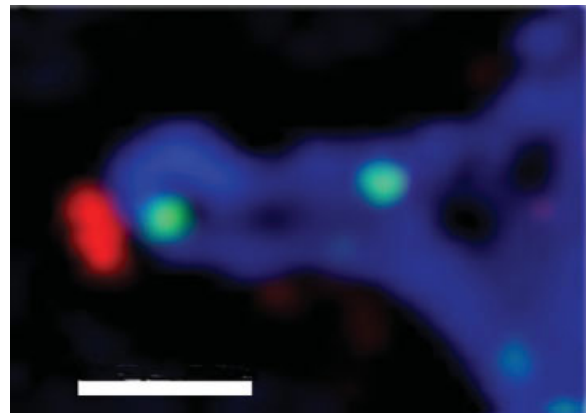


Figure 3 tPA-EYFP is present in synapsed spines. De-blurred fluorescence image of a synapse derived from a 17-DIV hippocampal neuron expressing tPA-EYFP (yellow) and ECFP (blue) and immunostained for synapsin I (red). Two tPA-EYFP-containing DCGs appear in the postsynaptic region; one of these DCGs is positioned in the head of the spine, directly apposed to the presynaptic marker synapsin I, whereas the other DCG is in the stalk of the spine. Bar = 1 μm .

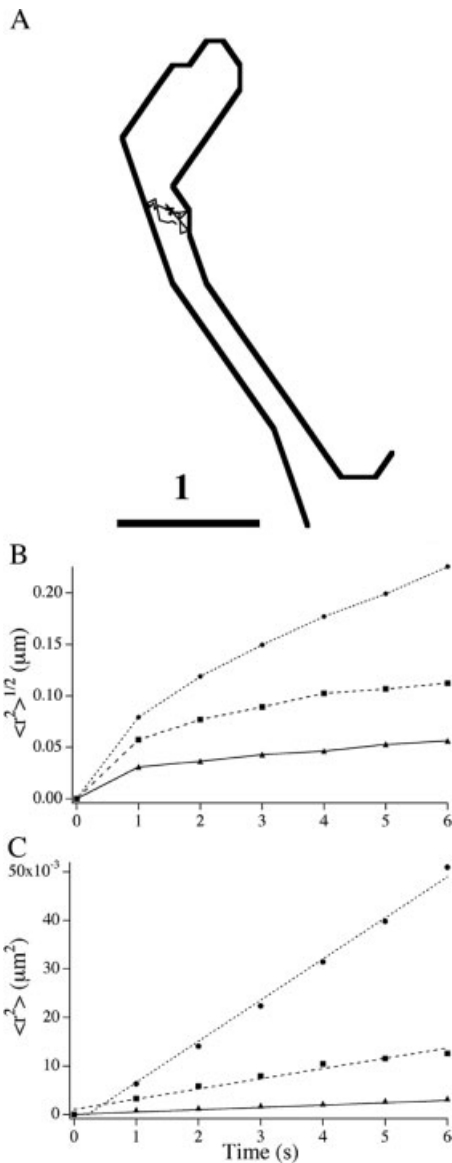


Figure 4 DCGs in spines are immobile or undergo slow, diffusive motion. (A) Trajectory, which shows changes in the position of the center-of-mass of a DCG in a spine, superimposed on an outline of the spine. Representative plots (B) of $\langle r^2 \rangle^{1/2}$ versus t , and (C) of $\langle r^2 \rangle$ versus t showing that DCGs in spines essentially are immobile or undergo slow, diffusive motion. The plot labeled with closed squares was derived from the trajectory shown in panel (A). Bar = 1 μm.

motion, $\langle r^2 \rangle$ varies linearly with t , implying that the motion of these DCGs was diffusive. Data derived from the tracking and quantification of DCGs in processes revealed that $\approx 50\%$ of the DCGs in processes underwent rapid and directed transport at an average speed of 0.46 ± 0.30 μm/s (SD) and that only $\approx 4\%$ were immobile ($n = 70$ DCGs).

tPA-EYFP Undergoes Partial, Calcium-Dependent Release from Dendritic Spines

Key unresolved issues surrounding tPA's role in memory formation include determining: (1) whether tPA is released from synapses, and (2) what conditions and mechanisms elicit this putative release.

To address some of these issues, we assayed for release of tPA-EYFP from spines of hippocampal

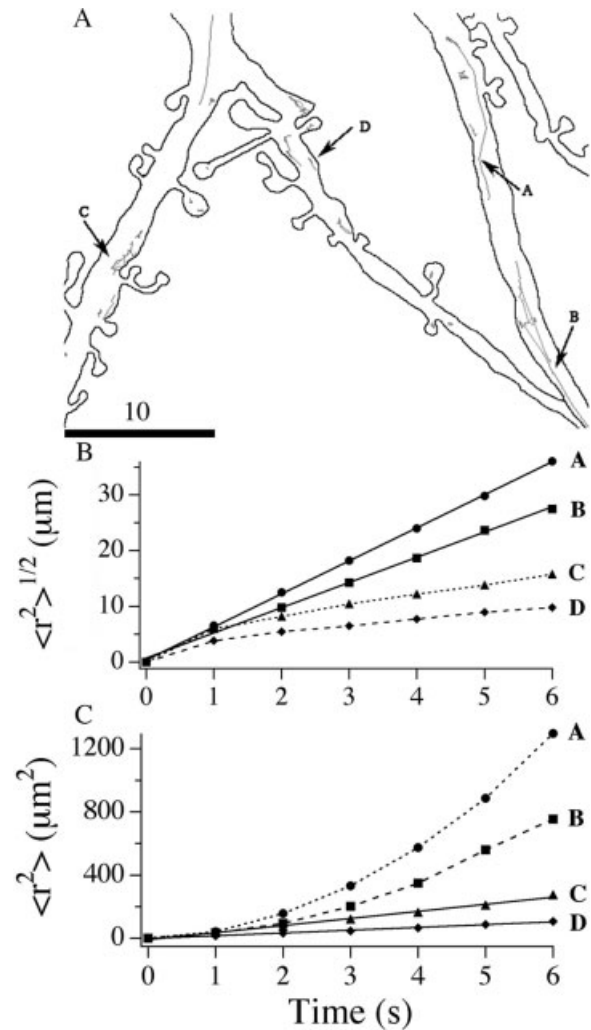


Figure 5 DCGs in processes are predominantly mobile and undergo rapid, directed motion. Trajectories (A) of DCGs in processes and spines, superimposed on an outline of the processes and spines. Representative plots (B) of $\langle r^2 \rangle^{1/2}$ versus t , and (C) of $\langle r^2 \rangle$ versus t showing that DCGs in processes undergo rapid, directed, and diffusive motion. Letters next to the plots identify the trajectories from which the plots were derived. In panels (B) and (C), values of $\langle r^2 \rangle^{1/2}$ and $\langle r^2 \rangle$ were multiplied by 3 and 10 for DCGs C and D. Bar = 10 μm.

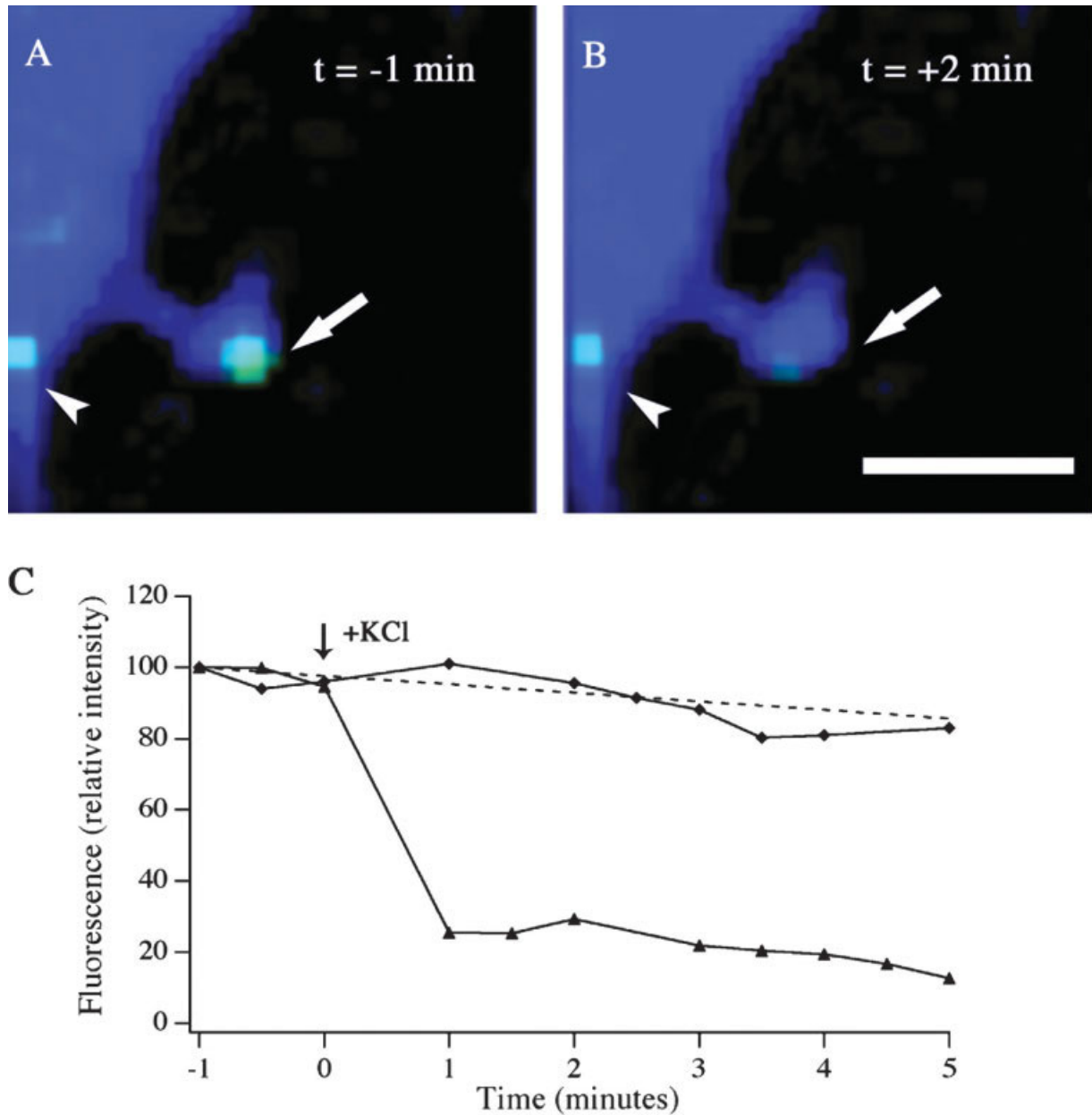


Figure 6 K^+ -induced depolarization induces postsynaptic release of tPA-EYFP. Deblurred fluorescence images of a tPA-EYFP-containing DCG in the head of a dendritic spine [arrow in panels (A) and (B)] (A) at 1.0 min prior to, and (B) at 2.0 min following the addition of 50 mM KCl. Also shown is a tPA-EYFP-containing DCG in the adjacent dendritic process [arrowhead in panels (A) and (B)], which fails to release tPA-EYFP in response to the depolarizing stimulus. Temporal dependences (C) of the fluorescence signals from the tPA-EYFP-containing DCGs localized in the dendritic spine (▲) and in the dendritic process (◆) before and after addition of 50 mM KCl. The depolarizing stimulus was applied at the zero time point. The dashed line represents the average loss of fluorescence signal due to photobleaching. Bar = 2 μ m.

neurons. We adopted standard assays and measured loss of fluorescence induced by depolarization with high KCl (Burke et al., 1997; Lang et al., 1997; Hartmann et al., 2001). Figure 6(A,B) shows images of a DCG containing tPA-EYFP in a spine before and

after addition of high KCl, and Figure 6(C) shows the time-course of the total fluorescence emitted from this DCG before and after addition of high KCl. For this DCG, loss of fluorescence reached a plateau over a time-scale of ≈ 1 min and was $\approx 75\%$.

Importantly, Figure 6(A,B) also shows images of a DCG containing tPA-EYFP in a dendritic process before and after addition of high KCl. Unlike the DCG in the nearby spine, the DCG in the process underwent a relatively slow, monotonic, and small ($\approx 17\%$) change in fluorescence intensity over a 5 min period, as shown by the second time-course in Figure 6(C). This suggests that the intensity changes observed for the DCG in the spine did not arise purely from photobleaching, or from a loss of cell viability or from damage to the plasma membrane.

The slow and relatively small fluorescence loss in Figure 6(C) most probably arose from photobleaching. To determine the effects of photobleaching quantitatively, we imaged DCGs in neurons in a low KCl buffer that did not elicit release, and we calculated average loss of fluorescence as a function of time. At the end of 5 min, average loss of fluorescence was $15.3 \pm 2.3\%$ (SEM) ($n = 29$ DCGs). We also used these average loss data to compute a best-fit line that describes average photobleaching as a function of time. This line is shown in Figure 6(C) and was used to correct some of our release data for the effects of photobleaching, similar to past work (Silverman et al., 2005).

The DCG in the spine in Figure 6(A) released a relatively large fraction of its tPA content over a time-scale of ≈ 1 min. To determine if this result was typical, we monitored release (loss of fluorescence) from 23 DCGs in spines in a high-KCl buffer. We computed loss over a 5 min period, because we found that tPA is released relatively slowly and that there can be a delay before the onset of tPA release, similar to past work (Taraska et al., 2003). In a high-KCl buffer, extent of fluorescence loss was variable, ranging from ≈ 25 – 87% and averaging $48.7 \pm 3.0\%$ (SEM), and was significantly larger than photobleaching-associated loss in a low-KCl buffer ($p \approx 10^{-11} < 0.05$; Student's t test). This variability is illustrated by the representative photobleaching-corrected release traces shown in Figure 7, which reveal that both the extent and the time to onset of release varied significantly.

To determine how much tPA is released from DCGs, we computed the range and average loss of fluorescence after correction for photobleaching. Losses corrected for photobleaching ranged from ≈ 12 – 74% and averaged $31.8 \pm 3.1\%$ (SEM) for the 23 DCGs examined.

Calcium plays a key role in initiating LTP and in initiating regulated exocytosis. Thus, we also studied the calcium dependence of the release of tPA-EYFP. In the absence of external Ca^{+2} , and in the presence of 5 mM EGTA, average loss of fluorescence after

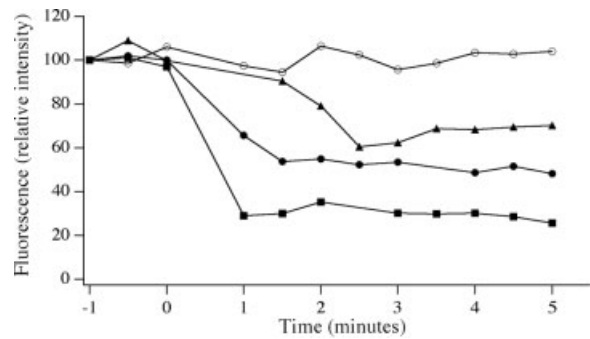


Figure 7 Depolarization-induced release of tPA-EYFP is partial and calcium dependent. Temporal dependences of the fluorescence signals from tPA-EYFP-containing DCGs in the presence (▲, ●, ■) and absence (○) of extracellular calcium before and after receipt of a depolarizing stimulus, which was applied at the zero time point.

addition of high-KCl averaged $13.2 \pm 1.5\%$ (SEM) ($n = 5$ DCGs) and was statistically indistinguishable from photobleaching-associated loss ($p = 0.4 > 0.05$). This is exemplified in the representative fluorescence trace shown in Figure 7 collected from neurons exposed to high KCl in the absence of Ca^{+2} .

DISCUSSION

The experiments described here were directed at: (1) determining if tPA localizes to, and is released from, postsynaptic sites in mature hippocampal neurons; (2) elucidating the conditions and mechanisms that elicit any postsynaptic release; and (3) relating the results to current models of tPA's role in LTP and to current models of regulated exocytosis.

Implications for Hypotheses about tPA's Localization and Release from Synapses

One commonly accepted idea is that learning and memory formation involve changes in the strength of specific synaptic connections, and that these changes are driven by the synthesis, and subsequent activity, of specific proteins (Kandel, 2001). As an outgrowth of this idea, secreted proteins (such as tPA) that function in learning often are postulated to undergo calcium-dependent release from synapses (Zhuo et al., 2000). This postulate is appealing because calcium influx plays a key role in initiating LTP and because protein secretion at synapses is an efficient way to initiate changes at synapses.

Although suggestive data exist, conclusive data establishing sites of synaptic localization and release of tPA have remained elusive (Fernandez-Monreal

et al., 2004b; Shin et al., 2004). To address these unresolved issues, we used a double-label system to visualize dendritic spines and tPA chimeras in mature hippocampal neurons. We focused on spines because tPA is hypothesized to be a postsynaptic communicator. Our system shows that tPA chimeras localize to DCGs in heads and stalks of dendritic spines and that tPA chimeras are released from spines in response to high-KCl-induced membrane depolarization, but only if Ca^{2+} is present in the external medium. Our results thus provide direct confirmation of two fundamental hypotheses about tPA that bear on its function in LTP.

We also used our system to elucidate the kinetics and extent of release of tPA at postsynaptic sites. We found that release occurs over a time-scale of minutes in response to high-KCl-induced depolarization, similar to BDNF (Hartmann et al., 2001; Kojima et al., 2001; Brigadski et al., 2005). We also found that tPA typically undergoes only partial release (averaging $\approx 32\%$) from DCGs in spines in response to high-KCl-induced depolarization. This suggests that the tPA content of individual DCGs is available for release for several cycles of postsynaptic depolarization, given that DCGs are retained in spines for long amounts of time. Importantly, partial release provides a potential mechanism to avoid depletion of tPA at postsynaptic sites and to regulate the amount of tPA release.

Implications for Interactions of tPA with Putative Substrates

Some uncertainty surrounds tPA's precise function at synapses (Fernandez-Monreal et al., 2004b; Shin et al., 2004). One prominent idea is that tPA (perhaps in conjunction with plasmin) influences LTP by cleaving relevant substrates. For example, tPA/plasmin may cleave molecules that mediate adhesion at synapses and thereby facilitate structural changes at synapses that underlie memory formation. Consistent with this, the tPA-plasmin system can cleave neural cell adhesion molecules that form adhesive linkages between neurons, as well as between neurons and the extracellular matrix (Endo et al., 1999).

tPA may also influence LTP by cleaving other substrates. For example, tPA may be involved in cleaving proBDNF at synapses to produce BDNF, another protein that plays a key role in LTP. Consistent with this, plasmin converts proBDNF into BDNF in the hippocampus following tPA-mediated conversion of plasminogen into plasmin, and this activation cascade is important for the maintenance of L-LTP (Pang et al., 2004). Alternatively, or in addition, tPA may cleave the NMDA receptor, and thereby alter

NMDA receptor signaling and induction of LTP (Centonze et al., 2002).

Our data impact current ideas about the identity of tPA's substrates at synapses. For example, we have shown that tPA is present in hippocampal neurons in DCGs containing SgII that localize to postsynaptic sites; this also is true of proBDNF (Hartmann et al., 2001; Kojima et al., 2001; Brigadski et al., 2005), strongly suggesting that tPA and proBDNF colocalize in the same secretory organelles at postsynaptic sites in hippocampal neurons. We also have shown that these organelles undergo regulated exocytosis from spines, strongly supporting the corelease of tPA and proBDNF at the postsynaptic plasma membrane. Importantly, this corelease will ensure that tPA and proBDNF are strategically positioned to engage in a postsynaptic activation cascade involving plasmin. Release of tPA at the postsynaptic plasma membrane also facilitates interaction with the NMDA receptor, which is housed in the postsynaptic plasma membrane.

Attributes and Implications of DCG Mobility in Spines

Recently, considerable effort and interest have been directed at elucidating DCG dynamics. In large part this effort and interest stem from the fact that dynamics can influence important attributes of DCG exocytosis, including the slow and limited release of DCG cargo (Burke et al., 1997; Abney et al., 1999).

Two neuroendocrine systems have dominated past studies of DCG dynamics. The first system is the growth cone of the PC12 cell. DCGs in growth cones of PC12 cells are predominantly mobile, undergoing slow diffusive transport (Burke et al., 1997; Abney et al., 1999; Han et al., 1999). The second system is the near-membrane region of the chromaffin cell. Unlike DCGs in growth cones of PC12 cells, membrane-proximal DCGs in chromaffin cells are largely immobile (Oheim et al., 1998; Johns et al., 2001). As discussed below, these attributes of dynamics have been linked to important attributes of DCG exocytosis.

Unlike neuroendocrine cells, relatively little effort has been directed at elucidating DCG dynamics in neurons, especially DCG dynamics at synapses, because neurons are more difficult to study (Shakiryanova et al., 2005). To elucidate this issue, we studied DCG dynamics in spines of hippocampal neurons. Our data show that most DCGs in spines are immobile, and that the mobile DCGs in spines undergo slow, diffusive transport. In this respect, DCGs in spines of hippocampal neurons are markedly different from DCGs in growth cones of PC12 cells and hippo-

campal neurons, whereas they are similar to DCGs in presynaptic termini of *Drosophila* neuromuscular junctions under basal conditions (Shakiryanova et al., 2005). These data suggest that DCGs become immobilized as growth cones mature into synapses.

We also studied DCG dynamics in spines before exocytosis and found that exocytosis is preceded by relatively small-scale movement. In this respect, DCG in spines of hippocampal neurons again are markedly different from DCGs in growth cones. In growth cones, exocytosis is preceded by substantial movement (Silverman et al., 2005).

Previous work suggests that the slow and limited release of DCG cargo from growth cones of differentiated PC12 cells is a consequence of the heterogeneous diffusive mobility of DCGs in PC12 cells and substantial short-ranged transport prior to exocytosis (Abney et al., 1999; Ng et al., 2003). In contrast, our data suggest that the slow and limited release of tPA from spines of hippocampal neurons is a consequence of the slow and partial escape of tPA from DCGs. This latter explanation is supported by several attributes of our data including: (1) the fact that tPA release occurs over a relatively long time-scale after its onset; (2) the fact that only $\approx 32\%$ of tPA on average is released from individual DCGs; (3) the fact that DCGs in spines are predominantly immobile in both basal and stimulated neurons; and (4) the fact that exocytosis is preceded by relatively little movement.

Implications for Models of DCG Exocytosis

DCGs in neuroendocrine cells undergo exocytosis via several mechanisms that are distinguished by their extent of DCG-plasma membrane mixing (Ryan, 2003). One is the “fuse-and-collapse” mechanism, which is characterized by full collapse of the DCG membrane into the plasma membrane. In this case, DCG cargo is fully released and subsequent endocytotic retrieval processes involve extensive resorting of membrane components. Two alternatives are the “fuse-pinch-linger” and the “kiss-and-run” mechanisms, which are characterized by formation of a fusion pore but maintenance of the integrity and shape of the DCG. If the fusion pore closes through fission mediated by dynamin, the mechanism is fuse-pinch-linger (Ryan, 2003); in contrast, if the fusion pore closes rapidly (within a few seconds) and directly, the mechanism is kiss-and-run (Klyachko and Jackson, 2002; Palfrey and Artalejo, 2003). These latter two mechanisms can lead to partial release of DCG cargo, and they bypass the need for extensive endocytotic resorting.

Unlike in neuroendocrine cells, the mechanisms underlying DCG exocytosis and regulated protein release in neurons largely remain a mystery. In particular, it is not known if DCGs in neurons utilize the fuse-and-collapse, fuse-pinch-linger, kiss-and-run (or alternative) mechanisms.

To elucidate this issue, we monitored the time-scale and extent of release of tPA-EYFP from DCGs in spines. Our data strongly suggest that these DCGs do not undergo exocytosis via the fuse-and-collapse or the kiss-and-run mechanisms. This is supported by several attributes of our data, particularly: (1) the fact that tPA-EYFP is released over a relatively long time-scale (≈ 1 min); (2) the fact that “intact” DCGs releasing tPA-EYFP are visible in spines for at least 10 min; and (3) the fact that release of tPA-EYFP generally is incomplete. Rather, our data suggest that DCGs containing tPA-EYFP in spines undergo exocytosis via a mechanism, such as fuse-pinch-linger, that permits partial release and reuse of DCG cargo but that does not involve very rapid closure of the fusion pore.

Implications for tPA Biogenesis and Trafficking to Spines

Recent data suggest that tPA is synthesized in both the soma and dendrites of hippocampal neurons (Shin et al., 2004). The latter, “synaptically local” synthesis is the focus of considerable current interest, because it may provide a mechanism for relatively rapidly and selectively delivering tPA to active synapses (Jiang and Schuman, 2002; Sutton and Schuman, 2005).

Recent data also suggest that dendritic synthesis of tPA occurs in only a subset of dendrites, because only a subset of dendrites contains Golgi (Horton and Ehlers, 2003). Given this, hippocampal neurons need additional mechanisms for rapidly and selectively delivering tPA to active spines. Interestingly, our data suggest one possibility: rapid dendritic transport of tPA in conjunction with the maintenance of a pool of DCGs containing tPA along dendritic processes. To quantify the temporal efficacy of rapid transport in the presence of a pool, we estimated the average distance between DCGs containing tPA and spines, and we estimated the time for transport to deliver DCGs containing tPA to spines. Images of the distribution of endogenous tPA in hippocampal neurons (Shin et al., 2004), and our images, suggest that the dendritic density of DCGs containing tPA is at least $1/(5 \mu\text{m})$. This implies that on average a spine will have a DCG within $\approx 2.5 \mu\text{m}$ of it. The associated time-scale for transport into spines, t , can be calculated using the relationship $\langle r^2 \rangle^{1/2} = vt$, where t is the time, $\langle r^2 \rangle^{1/2}$ is

the distance, and v is the speed (Berg, 1993). We calculate that $t \approx 5$ s, using the average DCG speed, $\approx 0.46 \mu\text{m/s}$, obtained here. This suggests that the pool of dendritic DCGs containing tPA can rapidly supply active spines.

Our data also suggest a mechanism that hippocampal neurons might use to avoid depleting tPA at active synapses. This mechanism is incomplete release of tPA from DCGs during exocytosis at spines in conjunction with long-term retention of DCGs in spines.

We thank Barbara Smoody of the Banker laboratory for extensive support with the culture of hippocampal neurons, and Dr. James Abney for a critical reading of this manuscript.

REFERENCES

- Abney JR, Meliza CD, Cutler B, Kingma M, Lochner JE, Scalettar BA. 1999. Real-time imaging of the dynamics of secretory granules in growth cones. *Biophys J* 77: 2887–2895.
- Alonso M, Medina JH, Pozzo-Miller L. 2004. ERK1/2 activation is necessary for BDNF to increase dendritic spine density in hippocampal CA1 pyramidal neurons. *Learn Mem* 11:172–178.
- Banker G, Goslin K. 1998. *Culturing Nerve Cells*. Cambridge, MA: MIT Press. 666 p.
- Baranes D, Lederfein D, Huang YY, Chen M, Bailey CH, Kandel ER. 1998. Tissue plasminogen activator contributes to the late phase of LTP and to synaptic growth in the hippocampal mossy fiber pathway. *Neuron* 21:813–825.
- Berg H. 1993. *Random Walks in Biology*. Princeton, NJ: Princeton University Press. 164 p.
- Brigadski T, Hartmann M, Lessmann V. 2005. Differential Vesicular Targeting and Time Course of Synaptic Secretion of the Mammalian Neurotrophins. *J Neurosci* 25:7601–7614.
- Burke NV, Han W, Li D, Takimoto K, Watkins SC, Levitan ES. 1997. Neuronal peptide release is limited by secretory granule mobility. *Neuron* 19:1095–1102.
- Centonze D, Napolitano M, Saulle E, Gubellini P, Picconi B, Martorana A, Pisani A, et al. 2002. Tissue plasminogen activator is required for corticostriatal long-term potentiation. *Eur J Neurosci* 16:713–721.
- Davies BJ, Pickard BS, Steel M, Morris RG, Lathe R. 1998. Serine proteases in rodent hippocampus. *J Biol Chem* 273: 23004–23011.
- Endo A, Nagai N, Urano T, Takada Y, Hashimoto K, Takada A. 1999. Proteolysis of neuronal cell adhesion molecule by the tissue plasminogen activator-plasmin system after kainate injection in the mouse hippocampus. *Neurosci Res* 33:1–8.
- Fernandez-Monreal M, Lopez-Atalaya JP, Benchenane K, Cacquevel M, Dulin F, Le Caer JP, Rossier J, et al. 2004a. Arginine 260 of the amino-terminal domain of NR1 subunit is critical for tissue-type plasminogen activator-mediated enhancement of N-methyl-D-aspartate receptor signaling. *J Biol Chem* 279:50850–50856.
- Fernandez-Monreal M, Lopez-Atalaya JP, Benchenane K, Leveille F, Cacquevel M, Plawinski L, MacKenzie ET, et al. 2004b. Is tissue-type plasminogen activator a neuromodulator? *Mol Cell Neurosci* 25:594–601.
- Frey U, Muller M, Kuhl D. 1996. A different form of long-lasting potentiation revealed in tissue plasminogen activator mutant mice. *J Neurosci* 16:2057–2063.
- Gualandris A, Jones TE, Strickland S, Tsirka SE. 1996. Membrane depolarization induces calcium-dependent secretion of tissue plasminogen activator. *J Neurosci* 16:2220–2225.
- Guzowski JF, Lyford GL, Stevenson GD, Houston FP, McGaugh JL, Worley PF, Barnes CA. 2000. Inhibition of activity-dependent arc protein expression in the rat hippocampus impairs the maintenance of long-term potentiation and the consolidation of long-term memory. *J Neurosci* 20:3993–4001.
- Han W, Ng YK, Axelrod D, Levitan ES. 1999. Neuropeptide release by efficient recruitment of diffusing cytoplasmic secretory vesicles. *Proc Natl Acad Sci USA* 96: 14577–14582.
- Hartmann M, Heumann R, Lessmann V. 2001. Synaptic secretion of BDNF after high-frequency stimulation of glutamatergic synapses. *EMBO J* 20:5887–5897.
- Haubensak W, Narz F, Heumann R, Lessmann V. 1998. BDNF-GFP containing secretory granules are localized in the vicinity of synaptic junctions of cultured cortical neurons. *J Cell Sci* 111:1483–1493.
- Henkel AW, Simpson LL, Ridge RM, Betz WJ. 1996. Synaptic vesicle movements monitored by fluorescence recovery after photobleaching in nerve terminals stained with FM1-43. *J Neurosci* 16:3960–3967.
- Hiraoka Y, Swedlow JR, Paddy MR, Agard DA, Sedat JW. 1991. Three-dimensional multiple-wavelength fluorescence microscopy for the structural analysis of biological phenomena. *Semin Cell Biol* 2:153–165.
- Ho DY. 1994. Amplicon-based herpes simplex virus vectors. *Methods Cell Biol* 43 Pt A:191–210.
- Hoffman KB, Martinez J, Lynch G. 1998. Proteolysis of cell adhesion molecules by serine proteases: a role in long term potentiation? *Brain Res* 811:29–33.
- Horton AC, Ehlers MD. 2003. Dual modes of endoplasmic reticulum-to-Golgi transport in dendrites revealed by live-cell imaging. *J Neurosci* 23:6188–6199.
- Huang YY, Bach ME, Lipp HP, Zhuo M, Wolfer DP, Hawkins RD, Schoonjans L, et al. 1996. Mice lacking the gene encoding tissue-type plasminogen activator show a selective interference with late-phase long-term potentiation in both Schaffer collateral and mossy fiber pathways. *Proc Natl Acad Sci USA* 93:8699–8704.
- Jiang C, Schuman EM. 2002. Regulation and function of local protein synthesis in neuronal dendrites. *Trends Biochem Sci* 27:506–513.
- Johns LM, Levitan ES, Shelden EA, Holz RW, Axelrod D. 2001. Restriction of secretory granule motion near the plasma membrane of chromaffin cells. *J Cell Biol* 153: 177–190.

- Kandel ER. 2001. The molecular biology of memory storage: a dialogue between genes and synapses. *Science* 294:1030–1038.
- Klyachko VA, Jackson MB. 2002. Capacitance steps and fusion pores of small and large-dense-core vesicles in nerve terminals. *Nature* 418:89–92.
- Kojima M, Takei N, Numakawa T, Ishikawa Y, Suzuki S, Matsumoto T, Katoh-Semba R, et al. 2001. Biological characterization and optical imaging of brain-derived neurotrophic factor-green fluorescent protein suggest an activity-dependent local release of brain-derived neurotrophic factor in neurites of cultured hippocampal neurons. *J Neurosci Res* 64:1–10.
- Kraszewski K, Daniell L, Mundigl O, De Camilli P. 1996. Mobility of synaptic vesicles in nerve endings monitored by recovery from photobleaching of synaptic vesicle-associated fluorescence. *J Neurosci* 16:5905–5913.
- Kraszewski K, Mundigl O, Daniell L, Verderio C, Matteoli M, De Camilli P. 1995. Synaptic vesicle dynamics in living cultured hippocampal neurons visualized with CY3-conjugated antibodies directed against the lumenal domain of synaptotagmin. *J Neurosci* 15:4328–4342.
- Lang T, Wacker I, Steyer J, Kaether C, Wunderlich I, Soldati T, Gerdes HH, et al. 1997. Ca²⁺-triggered peptide secretion in single cells imaged with green fluorescent protein and evanescent-wave microscopy. *Neuron* 18:857–863.
- Lessmann V, Gottmann K, Heumann R. 1994. BDNF and NT-4/5 enhance glutamatergic synaptic transmission in cultured hippocampal neurons. *NeuroReport* 6:21–25.
- Levine ES, Dreyfus CF, Black IB, Plummer MR. 1995. Brain-derived neurotrophic factor rapidly enhances synaptic transmission in hippocampal neurons via postsynaptic tyrosine kinase receptors. *Proc Natl Acad Sci USA* 92:8074–8077.
- Li YX, Zhang Y, Lester HA, Schuman EM, Davidson N. 1998. Enhancement of neurotransmitter release induced by brain-derived neurotrophic factor in cultured hippocampal neurons. *J Neurosci* 18:10231–10240.
- Lochner JE, Kingma M, Kuhn S, Meliza CD, Cutler B, Scalettar BA. 1998. Real-time imaging of the axonal transport of granules containing a tissue plasminogen activator/green fluorescent protein hybrid. *Mol Biol Cell* 9:2463–2476.
- Madani R, Hulo S, Toni N, Madani H, Steimer T, Muller D, Vassalli JD. 1999. Enhanced hippocampal long-term potentiation and learning by increased neuronal expression of tissue-type plasminogen activator in transgenic mice. *EMBO J* 18:3007–3012.
- Matys T, Strickland S. 2003. Tissue plasminogen activator and NMDA receptor cleavage. *Nat Med* 9:371–372; author reply 372–373.
- Medina MG, Ledesma MD, Dominguez JE, Medina M, Zafra D, Alameda F, Dotti CG, et al. 2005. Tissue plasminogen activator mediates amyloid-induced neurotoxicity via Erk1/2 activation. *EMBO J* 24:1706–1716.
- Nakagami Y, Abe K, Nishiyama N, Matsuki N. 2000. Laminin degradation by plasmin regulates long-term potentiation. *J Neurosci* 20:2003–2010.
- Ng YK, Lu X, Gulacsi A, Han W, Saxton MJ, Levitan ES. 2003. Unexpected mobility variation among individual secretory vesicles produces an apparent refractory neuro-peptide pool. *Biophys J* 84:4127–4134.
- Nicole O, Docagne F, Ali C, Margaille I, Carmeliet P, MacKenzie ET, Vivien D, et al. 2001. The proteolytic activity of tissue-plasminogen activator enhances NMDA receptor-mediated signaling. *Nat Med* 7:59–64.
- Oheim M, Loerke D, Stuhmer W, Chow RH. 1998. The last few milliseconds in the life of a secretory granule. Docking, dynamics and fusion visualized by total internal reflection fluorescence microscopy (TIRFM). *Eur Biophys J* 27:83–98.
- Palfrey HC, Artalejo CR. 2003. Secretion: kiss and run caught on film. *Curr Biol* 13:R397–399.
- Pang PT, Teng HK, Zaitsev E, Woo NT, Sakata K, Zhen S, Teng KK, et al. 2004. Cleavage of proBDNF by tPA/plasmin is essential for long-term hippocampal plasticity. *Science* 306:487–491.
- Patterson SL, Abel T, Deuel TA, Martin KC, Rose JC, Kandel ER. 1996. Recombinant BDNF rescues deficits in basal synaptic transmission and hippocampal LTP in BDNF knockout mice. *Neuron* 16:1137–1145.
- Pawlak R, Magarinos AM, Melchor J, McEwen B, Strickland S. 2003. Tissue plasminogen activator in the amygdala is critical for stress-induced anxiety-like behavior. *Nat Neurosci* 6:168–174.
- Qian Z, Gilbert ME, Colicos MA, Kandel ER, Kuhl D. 1993. Tissue-plasminogen activator is induced as an immediate-early gene during seizure, kindling and long-term potentiation. *Nature* 361:453–457.
- Ryan TA. 2003. Kiss-and-run, fuse-pinch-and-linger, fuse-and-collapse: the life and times of a neurosecretory granule. *Proc Natl Acad Sci USA* 100:2171–2173.
- Salles FJ, Strickland S. 2002. Localization and regulation of the tissue plasminogen activator-plasmin system in the hippocampus. *J Neurosci* 22:2125–2134.
- Sappino AP, Madani R, Huarte J, Belin D, Kiss JZ, Wohlwend A, Vassalli JD. 1993. Extracellular proteolysis in the adult murine brain. *J Clin Invest* 92:679–685.
- Saxton MJ, Jacobson K. 1997. Single-particle tracking: applications to membrane dynamics. *Annu Rev Biophys Biomol Struct* 26:373–399.
- Scalettar BA, Swedlow JR, Sedat JW, Agard DA. 1996. Dispersion, aberration and deconvolution in multi-wavelength fluorescence images. *J Microsc* 182:50–60.
- Seeds NW, Basham ME, Ferguson JE. 2003. Absence of tissue plasminogen activator gene or activity impairs mouse cerebellar motor learning. *J Neurosci* 23:7368–7375.
- Seeds NW, Williams BL, Bickford PC. 1995. Tissue plasminogen activator induction in Purkinje neurons after cerebellar motor learning. *Science* 270:1992–1994.
- Shakiryanova D, Tully A, Hewes RS, Deitcher DL, Levitan ES. 2005. Activity-dependent liberation of synaptic neuro-peptide vesicles. *Nat Neurosci* 8:173–178.
- Shin CY, Kundel M, Wells DG. 2004. Rapid, activity-induced increase in tissue plasminogen activator is mediated by metabotropic glutamate receptor-dependent mRNA translation. *J Neurosci* 24:9425–9433.

- Silverman MA, Johnson S, Gurkins D, Farmer M, Lochner JE, Rosa P, Scalettar BA. 2005. Mechanisms of transport and exocytosis of dense-core granules containing tissue plasminogen activator in developing hippocampal neurons. *J Neurosci* 25:3095–3106.
- Sutton MA, Schuman EM. 2005. Local translational control in dendrites and its role in long-term synaptic plasticity. *J Neurobiol* 64:116–131.
- Taraska JW, Perrais D, Ohara-Imaizumi M, Nagamatsu S, Almers W. 2003. Secretory granules are recaptured largely intact after stimulated exocytosis in cultured endocrine cells. *Proc Natl Acad Sci USA* 100:2070–2075.
- Tyler WJ, Pozzo-Miller L. 2003. Miniature synaptic transmission and BDNF modulate dendritic spine growth and form in rat CA1 neurones. *J Physiol* 553:497–509.
- Tyler WJ, Pozzo-Miller LD. 2001. BDNF enhances quantal neurotransmitter release and increases the number of docked vesicles at the active zones of hippocampal excitatory synapses. *J Neurosci* 21:4249–4258.
- Withers GS, Higgins D, Charette M, Banker G. 2000. Bone morphogenetic protein-7 enhances dendritic growth and receptivity to innervation in cultured hippocampal neurons. *Eur J Neurosci* 12:106–116.
- Wu GY, Deisseroth K, Tsien RW. 2001. Spaced stimuli stabilize MAPK pathway activation and its effects on dendritic morphology. *Nat Neurosci* 4:151–158.
- Wu YP, Siao CJ, Lu W, Sung TC, Frohman MA, Milev P, Bugge TH, et al. 2000. The tissue plasminogen activator (tPA)/plasmin extracellular proteolytic system regulates seizure-induced hippocampal mossy fiber outgrowth through a proteoglycan substrate. *J Cell Biol* 148:1295–1304.
- Zenisek D, Steyer JA, Almers W. 2000. Transport, capture and exocytosis of single synaptic vesicles at active zones. *Nature* 406:849–854.
- Zhuo M, Holtzman DM, Li Y, Osaka H, DeMaro J, Jacquin M, Bu G. 2000. Role of tissue plasminogen activator receptor LRP in hippocampal long-term potentiation. *J Neurosci* 20:542–549.